

**Topology of the microsomal glycerol-3-phosphate acyltransferase Gpt2p/Gat1p  
of *Saccharomyces cerevisiae***

*Martin Pagac*<sup>1,2,3</sup>, *Hector M. Vazquez*<sup>1</sup>, *Arlette Bochud*<sup>1</sup>, *Carole Roubaty*<sup>1,3</sup>, *Cécile Knöpfli*<sup>1</sup>,  
*Christine Vionnet*<sup>1</sup>, and *Andreas Conzelmann*<sup>1</sup>

<sup>1</sup>Department of Biology, University of Fribourg, CH-1700 Fribourg, Switzerland;

<sup>2</sup>Present address: College of Pharmacy, University of Hawaii, Hilo, USA

<sup>3</sup>These authors contributed equally to the work.

Correspondence: andreas.conzelmann@unifr.ch, Phone ++41263008631, Fax ++41263009735,

Running head: Topology of GPATs in yeast

**Key words not in title:**

Dual topology reporter; cysteine accessibility; phosphatidic acid; lyso-phosphatidic acid: acyl-Coenzyme A; microsomes.

## Summary

All glycerophospholipids are made from phosphatidic acid, which, according to the traditional view, is generated at the cytosolic surface of the ER. In yeast, phosphatidic acid is synthesized *de novo* by two acyl-CoA dependent acylation reactions. The first is catalyzed by one of the two homologous glycerol-3-phosphate acyltransferases Gpt2p/Gat1p and Sct1p/Gat2p, the second by one of the two 1-acyl-sn-glycerol-3-phosphate acyltransferases Slc1p and Ale1p/Slc4p. To study the biogenesis and topology of Gpt2p we observed the location of dual topology reporters inserted after various transmembrane helices. Moreover, using microsomes, we probed the accessibility of natural and substituted cysteine residues to a membrane impermeant alkylating agent and tested the protease sensitivity of various epitope tags inserted into Gpt2p. Finally, we assayed the sensitivity of the acyltransferase activity to membrane impermeant agents targeting lysine residues. By all these criteria we find that the most conserved motifs of Gpt2p and its functionally relevant lysines are oriented towards the ER lumen. Thus, the first step in biosynthesis of phosphatidic acid in yeast seems to occur in the ER lumen and substrates may have to cross the ER membrane.

182 words

## Introduction

Many eukaryotic lipids are made from phosphatidic acid (PA), a central metabolite, which is used in the various pathways generating polar membrane glycerophospholipids and triacylglycerols (Coleman and Lee, 2004). In yeast, PA is synthesized *de novo* through the acylation of L-glycerol-3-phosphate (G3P) by one of the glycerol-3-phosphate acyltransferases (GPATs) Gpt2p and Sct1p (Zheng and Zou, 2001; Zaremborg and McMaster, 2002), and subsequent acylation of the thus generated *lyso*-PA by a *lyso*-PA acyltransferase (LPAT) Slc1p or Ale1p/Slc4p (Fig. 1). Although having distinct physiological roles (Marr et al., 2012), Gpt2p and Sct1p are functionally redundant in the sense that *gpt2Δ sct1Δ* are not viable whereas singly deleted strains grow normally. The GPATs *GPT2*, *SCT1* and the LPAT *SLC1* are related and belong to the two cd07992 and cd07989 families within the lysophospholipid acyltransferase superfamily ([www.ncbi.nlm.nih.gov/Structure/cdd/cdd.shtml](http://www.ncbi.nlm.nih.gov/Structure/cdd/cdd.shtml)). They are characterized by the presence of 4 conserved sequence motifs, motifs I, II, III and IV (Lewin et al., 1999; Coleman and Lee, 2004; Shindou and Shimizu, 2009). Of these, motif I is the most stringently conserved while motif IV often is absent. These motifs are comprised within a 100-150 amino acids long acyltransferase domain defined by several motif databases (pfam01553, COG0204, smart00563). Motifs I, II and III are thought to form a surface pocket accommodating G3P based on the crystal structure of a related acyltransferase, the soluble chloroplast GPAT of *Cucurbita moschata* belonging to the acyltransferase family cd07985 (Slabas et al., 2002; Tamada et al., 2004).

It is currently believed that the biosynthesis of PA occurs at the cytosolic side of the bacterial plasma membrane and of the eukaryotic ER membrane (Bell et al., 1981; Coleman and Lee, 2004; Alberts et al., 2008). Here we investigate the membrane topology of the yeast GPATs, which catalyze the key reaction for PA and triacylglycerol biosynthesis. The data support an ER luminal location of motifs I, II and III of Gpt2p.

## Results

### *Topology of the yeast GPAT Gpt2p probed by dual topology reporters*

Gpt2p contributes the major part of GPAT activity of yeast (Zheng and Zou, 2001). Of its 6 hydrophobic stretches, 3 are uniformly predicted to be transmembrane helices (TMs) by all TOPCONS TM prediction algorithms, namely TMs 4, 5 and 6 (Fig. 2A, B). TM1 has a negative  $\Delta G_{mi}$  for membrane insertion ( $\Delta G_{mi}$ ) and is predicted by most algorithms as well as the global TOPCONS prediction, whereas TM2 and TM3 have  $\Delta G_{mi}$  values of +1.63 and +2.05 kcal/mol and are only predicted as a TM by some algorithms (Fig. 2A, B). (Strong hydrophobicity of sufficient length results in negative  $\Delta G_{mi}$  values). Motifs I, II and III all lie between TM1 and the questionable TM2. The ability of the various predicted TM domains to

bring the peptide chain into and through the ER membrane was investigated by making C-terminally truncated versions of *GPT2* carrying at their C terminal end a *SUC2-HIS4C* dual topology reporter (DTR) (Kim et al., 2003). Its invertase (Suc2p) fragment is N-glycosylated only when localized in the ER lumen, its His4Cp fragment complements the His auxotrophy of *his4Δ* cells only when located in the cytoplasm.

DTRs were inserted into Gpt2p downstream of TM1, namely between motifs I and II (at P109 and K120), close to motif III (at P259 and G262) and downstream of TM2 (at P333). Amongst these, the insertion at P333 can only indicate a transient position of loop L2-3 during the membrane insertion process, since, as detailed in the Discussion, only DTRs inserted at a minimal distance after strongly hydrophobic sequences of adequate length are able to predict the final topology of a given loop correctly (Cassel et al., 2008). Therefore, only the DTRs inserted between TM1 and TM2 can be considered to be relevant for the final topology of Gpt2p. These DTRs were all glycosylated and did provide relatively little His prototrophy to *his4Δ* cells (Fig. 2D). Thus, we interpret our data to say that the hydrophilic loop between TM1 and TM2 (L1-2) resides in the ER lumen not only at a certain stage during the biosynthesis of Gpt2p but probably also in the mature protein, as depicted in Fig. 2C. On the other hand the DTR in Gpt2p-P333-DTR is inserted after the questionable TM2 ( $\Delta G_{mi} = + 1.63$  kcal/mol) of Fig. 2C. The glycosylation of this construct suggests that during biosynthesis the first amino acids of loop L2-3 may reside in the ER lumen but this result cannot make an argument about the final location of the entire loop. Indeed, data below will argue that loop L2-3 finally ends up in the cytosol. In contrast to other constructs, Gpt2p-P467-DTR is not glycosylated (Fig. 2D). In this case the DTR is inserted into the middle of TM4, a TM that follows immediately after the questionable TM3 ( $\Delta G_{mi} = + 2.05$ ). Thus, the DTR at P467 also is not of the kind that allows making any predictions on the final topology, but it here serves as a control for a cytosolic DTR localization.

#### ***Cysteine accessibility indicates a luminal position of presumed active site residues***

The topology of membrane proteins can be studied by adding membrane impermeant alkylating agents to intact cells or isolated organelles before or after addition of detergent and observing which ones amongst the natural or artificially introduced cysteines of a given membrane protein get derivatized (Bogdanov et al., 2005; Guo et al., 2005). The preferred way is to utilize target proteins, which are functional and contain only one cysteine or at least, only one cysteine that is accessible to the derivatizing agent. Indeed, cysteines often are buried, *i.e.* not accessible from either side of the membrane, either because they are hidden inside the secondary, tertiary or quaternary structure of a cytosolic or extracytosolic loop, or else, because they are located in the hydrophobic core of the membrane, where the

alkylating reaction does not take place since it requires water. The ER membrane is reported to be more permeable than other cellular membranes (Le Gall et al., 2004) and we found that even PEG-mal can penetrate the ER membrane, especially at room temperature (Fig. S1A). We therefore probed microsomes using ubiquitin-maleimide (UBI-mal), a cysteine alkylating agent that increases the mass of proteins by about 9 kDa per derivatized cysteine and is completely impermeant (Fig. S1B)(Pagac et al., 2011).

We could replace each of the 8 cysteines of Gpt2p individually by Ser without destroying the enzyme activity but a *gpt2* allele having all 8 Cys replaced was non-functional (not shown). Cys 77, 254 and 297 are the most conserved Cys residues and alleles harboring one of these with the other 7 deleted were also nonfunctional except for Gpt2p-7CS-C77-V5-His<sub>6</sub>, which could rescue *gpt2Δ sct1Δ* cells when strongly overexpressed (Fig. S2A). The C77 of this construct was not accessible to UBI-mal (not shown). A construct retaining the three most conserved Cys residues (Gpt2p-5CS-C77-254-297-V5-His<sub>6</sub>) however rescued cells even when cells were grown on glucose (Figs. 3A, S3B, S3C), a condition, in which the Gpt2 protein was undetectable by Western blotting (not shown). Cysteine accessibility analysis of this C77-254-297 allele showed that all its residues are buried, since the three cysteines only become accessible in presence of the denaturing detergent SDS (Fig. 3A). Controls indicated that the luminal Kar2p and Gpi8p, containing 1 and 4 cysteines, respectively, were only derivatized by UBI-mal in the presence of detergent, demonstrating that the microsomes were tight (Fig. 3A'). We found that a *gpt2* allele retaining only cysteines 77, 110, 254 and 530 was also functional and had one Cys that became accessible after mild detergent treatment (Figs. 3B, 3B', S3C). As C77 and 254 are buried (see above), either 110 or 530 had to become accessible in detergent. When these two residues were tested individually, it turned out that Cys110 is buried whereas C530 is accessible (Figs. 3C, 3C', S3D), indicating that loop L5-6 is luminal as proposed in Fig. 2C.

Based on these preliminary results we chose to introduce further Cys residues into the *gpt2* allele retaining Cys 77, 254 and 297. Residues to be substituted by Cys in the *gpt2* C77-254-297 allele were chosen in highly exposed regions according to the NetSurfP predictor (<http://www.cbs.dtu.dk/services/NetSurfP>). We additionally asked that the substituted Cys would conserve a high surface exposure score (Table SIII). In this way, T99C, Q243C, H250C or T251C single mutations were introduced individually into the *gpt2* C77-254-297 allele. All resulting alleles rescued *gpt2Δ sct1Δ* cells as well as the parent allele (Fig. S3E). Cysteine accessibility tests showed that positions 99, 243 and 250 became accessible only after mild detergent solubilization, whereas position 251 remained buried (Fig. 3D, 3D'). The results suggest that loop L1-2 is luminal as proposed in Fig. 2C. The fact that C251 could not be derivatized may just indicate that the accessibility to side chains can change from one residue to

the next, as would be expected for instance for a  $\alpha$  helix, which lies at the surface of a globular protein.

We further probed the orientation of loop L2-3 by substituting in the *gpt2* C77-254-297 allele either single or three consecutive amino acids at highly exposed locations according to NetSurfP (Table SIII). These constructs also were functional (Fig. S4). As shown in Fig. 4A-C, one or two cysteines were accessible to UBI-mal already in the absence of mild detergent and the addition of detergent did not increase the accessibility of the cysteines at positions 330-332. These results argue that L2-3 is cytosolic although its first amino acids may transiently enter the lumen during biosynthesis as indicated by the luminal position of Gpt2p-P333-DTR.

### ***Topology of the Gpt2p probed by tag insertion into L1-2 and L2-3***

To further investigate the topology of the mature Gpt2p, we introduced HA- or VSVG-epitopes having net charges of -2 and 0 at neutral pH, respectively (Fig. 2C). Gpt2p-235-VSVG, Gpt2p-235-HA, Gpt2p-412-HA and Gpt2p-412-VSVG constructs, having epitopes inserted after amino acids 235 and 412, were functional, albeit the first two only if induced with galactose (Fig. S5A). Proteinase K treatment of microsomes of cells expressing Gpt2p-235-HA in the absence of detergent generated fragments of 69, 61, 44 and 25 kDa (Fig. 5A, lanes 3-5, 12-14). All these fragments were digested when Triton X-100 (TX-100) was present (lanes 6-8, 15-17). The 25-kDa fragment was the only one resistant to very high concentrations of protease (Fig. 5A, lane 14). It must comprise loop L1-2, TM1 and TM2, suggesting that the loop L1-2 is luminal but that L2-3 is cytosolic (Fig. 2C). The same results were obtained with Gpt2p-235-VSVG (Fig. 5B). As expected, the fragments generated by proteinase K from Gpt2p-235-VSVG and Gpt2p-235-HA had the same mobility on SDS-PAGE (Fig. S5B, lanes 4-7). The protease treatment of microsomes from cells expressing Gpt2p-412-VSVG indicated that the tag inserted after D412 was accessible for proteases to the same degree whether or not detergent was present (Fig. 5C, lanes 3-5 vs. 6-8; lanes 11-13 vs. lanes 14-16). In contrast, the luminal Gpi16p was protease sensitive only in presence of TX-100 (Fig. 5E, lane 13' vs. 16'). The protease sensitivity of Gpt2p-412-HA, as the one of Gpt2p-412-VSVG, was not influenced by the presence of detergent (Fig. 5D). These results reinforce the idea that the loop L2-3 in the mature protein is cytosolic, although the glycosylation of Gpt2p-P333-DTR suggests that the first amino acids of L2-3 may first be at the luminal side of the membrane during biosynthesis. The cytosolic location of L2-3 is all the more likely as Gpt2p-412-HA and Gpt2p-412-VSVG rescue *gpt2 $\Delta$  set1 $\Delta$*  cells even when the *GAL1* promoter is not induced. We conclude from these results that the most likely topology of Gpt2p is the one indicated by a continuous line in Fig. 2C and suggest that the relatively hydrophilic TM2 ( $\Delta G_{mi} = +1.63$  kcal/mol) may require more

downstream sequences than present in the Gpt2p-P333-DTR construct for correct membrane insertion.

#### ***Topological hints obtained from phosphoproteome***

Global proteome analysis by MS sequencing of peptides showed the presence of 8 phosphorylated Ser or Thr residues after TM6, between amino acids 632 and 693 of Gpt2p according to <http://www.phosphogrid.org/sites/34198>. Most of these phosphorylated residues (phosphosites) are part of recognition motifs of various cytosolic protein kinases. We also purified Gpt2p-V5-His<sub>6</sub> by Ni-affinity chromatography and excised the lower and upper band of Gpt2p from a preparative SDS-PAGE gel for MS analysis of tryptic peptides. As shown in Fig. S6, this analysis identified 5 of the 8 phosphosites reported in PhosphoGRID and also demonstrated with great confidence additional new sites at S2, Y315, T352 and S623 (Fig. 2C). Overall, we could not detect any phosphosites in the loops that are predicted to be luminal in the model of Fig. 2C although 81 % of the Ser and Thr residues of these loops were in peptides that were well detectable in the mass spectrometric analysis. Moreover, the phosphate at S2 places the N-terminus into the cytosol, phosphates Y315 and T352 confirm the cytosolic orientation of loop L2-3. Data also confirm the cytosolic orientation of the C-terminal end of Gpt2p, which was established by publicly available phosphosites and a global DTR approach before (Kim et al., 2006).

#### ***Functional assay suggests a luminal orientation of the active site in Gpt2p***

GPAT activity of Gpt2p can be assayed in microsomes of a *scf1Δ* strain using [<sup>14</sup>C]-G3P and unlabeled acyl-CoA as substrates using the microsomal assay characterized in Fig. S7. We went by the assumption that derivatization of lysines close to the substrate binding sites of Gpt2p has a higher probability of destroying the enzymatic activity than of lysines that are on the other side of the membrane. Thus we argued that, if indeed the conserved motifs I - III on the luminal side of the ER membrane form the substrate binding site for G3P, one might observe that impermeant lysine reactive agents would not touch the enzymatic activity unless the membrane barrier was removed using detergent. This indeed was found to be true. As shown in Fig. 6A, lane 1, during the GPAT assay little *lyso*-[<sup>14</sup>C]-PA was produced, since *lyso*-[<sup>14</sup>C]-PA was rapidly transformed into [<sup>14</sup>C]-PA by further acylation. However, [<sup>14</sup>C]-PA was not further metabolized, as expected, since the substrates for further biosynthetic steps are not present in the assay. The GPAT activity was similar in presence and absence of detergent (Fig. 6A and 6B, lanes 1 and 3; Fig. S7). When TNBS, an impermeant, lysine reactive reagent, was added to intact microsomes, the GPAT activity remained unchanged,

but more of the product appeared as *lyso*-PA (around 50% on average)(Fig. 6, lanes 4 and 5). The phenomenon may be explained by the fact that Slc1p, one of the two LPATs of yeast, is inactivated when lysine-reactive reagents are added to microsomes (Pagac et al., 2011). When TNBS was added together with detergent, the GPAT activity of Gpt2p was completely blocked (Fig. 6A and 6B, lanes 6, 7). Gpt2p contains 62 lysines, none of which is part of, or near one of the conserved motifs in the primary sequence, but it can be envisaged that the folding of the protein brings some lysines close to the catalytic pocket and that derivatization of such lysines blocks the enzyme. However, it cannot be excluded that the derivatization of some luminal lysines simply destabilizes the protein.

In summary, all our results argue that motifs I, II, and III of Gpt2p are in the lumen of the ER and support the notion that the active site of Gpt2p resides in the ER lumen. While the topology is not complete, our data nowhere contradicted the model proposed for Gpt2p by the TOPCONS integrated prediction (Fig. 2B, line f).

## Discussion

According to the textbook, microsomal GPATs and LPATs of eukaryotes have their active sites at the cytosolic surface of the ER (Alberts et al., 2008). If we presume that the conserved motifs I – III of Gpt2p form part of the active site, our data suggest that yeast may represent an exception to this rule. It is worth noting that yeast *GPT2* and *SCT1* are quite exceptional in that they have a bipartite PF01553 motif; a unique sequence (amino acids 138 to 232 in Gpt2p), not present in the large majority of microsomal GPATs, separates motif II from III. This sequence has not been recognized as a motif, *i.e.* it is not defined by any position specific score matrix (PSSM) in CDD. When performing a Blastp search at NCBI with this bisecting sequence of *GPT2*, one finds *SCT1* and only 16 other hits, all present in organisms belonging to the order of *saccharomycetales* and annotated as hypothetical proteins or putative GPATs. Thus, amino acids 138 to 232 of Gpt2p seem to set apart a small set of fungal microsomal GPATs. It is conceivable that this subset is also distinct by its topology, having motifs I – III in the ER lumen. Indeed, microsomal GPATs of man, mouse, *Xenopus laevis*, *Caenorhabditis elegans* and *Drosophila melanogaster* have a PF01553 acyltransferase motif, which is not bipartite, and all global and almost all specific TOPCONS algorithms for these metazoan acyltransferases predict a cytosolic location of motifs I, II, and III.

Our conclusions are based on concordant results obtained using a) DTR insertion, b) protease sensitivity of inserted tags, c) cysteine accessibility studies, d) phosphoproteomics and e) the ability of impermeant reagents to block the enzymatic function. Each one of these methods has inherent sources of potential error: a) In the past, topology reporter insertions have been utilized

to obtain topologies for many membrane proteins such as Sec61p, Pmt1p, Der3/Hrd1p, Lcb4p, Dpp1p, Lpp1p, Doa10p and Teb4 (Deak and Wolf, 2001; Strahl-Bolsinger and Scheinost, 1999; Wilkinson et al., 1996; Kihara et al., 2003; Kreft et al., 2006). However, the 3D crystal structures of multispan membrane proteins demonstrate that TMs can have positive  $\Delta G_{mi}$  values and that it also has been shown that the insertion of certain TMs with positive  $\Delta G_{mi}$  values is not strictly cotranslational, but delayed, and dependent on downstream sequences (Ott and Lingappa, 2002; Goder and Spiess, 2003; Hessa et al., 2007; Cassel et al., 2008; Buck et al., 2007; Pitonzo et al., 2009; Hedin et al., 2010; Kauko et al., 2010; Pitonzo et al., 2009). Therefore the location of DTRs following C-terminally truncated protein fragments is not necessarily indicative of the final location of the DTR-tagged loop but rather suggests its potential temporary position during membrane insertion of the protein (Pitonzo et al., 2009). Thus, a recent report indicates that the DTR insertion method yields reliable topology only if the reporter is inserted at a certain distance from a TM having a relatively high overall hydrophobicity and sufficient length to span the entire thickness of the membrane (Cassel et al., 2008). Similarly, DTR correctly predicted the position of loops following the strongly hydrophobic TMs 1, 3, 4, 6 and 8 of Sec61p but made wrong predictions for loops coming after TMs of lower hydrophobicity (Wilkinson et al., 1996; Junne et al., 2007). b) Tag insertions can change the orientation of hydrophilic loops and this has to be considered, even if the tagged enzyme remains active, since the activity may depend on a minor fraction of correctly folded protein having a different topology than the prevalent topology revealed by the biochemical methods. c) Cysteine accessibility assays in microsomes assume that cysteines, which are accessible only in presence of non-denaturing detergent, are located in the ER lumen. It however cannot be excluded that detergent solubilization slightly alters the enzyme structure such that cysteines close to the cytosolic surface or contacting membrane lipids become more accessible, while they are hidden in intact membranes. It however is likely that the substituted cysteines, on which our analysis most heavily relies, are not exposed by detergent deformation of Gpt2p, since they all reside in sequences, which are predicted to be much more exposed than the natural cysteines (Table SIII). e) The caveat described under c) could also apply to lysines, which may become more easily derivatized by TNBS in the presence of mild detergent and this may lead to the selective inhibition of enzyme activity observed in presence of detergent (Fig. 6). However, this would seem to be less of a problem in view of the fact that only 11 out of 61 lysines in Gpt2p are qualified as buried and the mean relative surface area of lysines in Gpt2p is 0.437, as opposed to 0.082 for cysteines, according to NetsurfP.

In spite of the methodological intricacies, all approaches used located the hydrophilic loop containing motifs I to III of Gpt2p to the lumen of the ER. Motif IV of Gpt2p is cytosolic according to our model (Fig. 2C). It however is likely that motif IV is not important for enzyme

catalysis (Zhang and Rock, 2008). Being merely defined as a proline surrounded by 5-7 hydrophobic amino acids, its identification in many instances is ambiguous (Lewin et al., 1999; Coleman and Lee, 2004) and it is poorly conserved ((Pagac et al., 2011), therein Fig. S2).

There are only few studies on the topology of mammalian GPATs. The GPAT activity is reported to be protease sensitive in rat liver microsomes (Coleman and Bell, 1978; Coleman and Bell, 1980; Bell et al., 1981). There also are two contradictory reports on *GPAT1* of the rat liver outer mitochondrial membrane, which place the N-terminal domain containing motifs I, II, III and IV in the cytosol (Gonzalez-Baro et al., 2001), or the intermembrane space (Balija et al., 2000), respectively. No mitochondrial GPATs have been described in *S. cerevisiae*.

Our data, at first sight, seem to suggest that yeast cells require a transporter importing acyl-CoA into the lumen of the ER. However, several other possibilities exist: a) The transport of acyl-CoA may be spontaneous. b) Luminal acyltransferases may work backwards generating acyl-CoA from triacylglycerols, glycerophospholipids or *lyso*-glycerophospholipids that are made or re-acylated by acyl-CoA dependent acyltransferases in the cytosolic leaflet of the ER and that can flop into the ER lumen. A human *SLC1*-orthologue indeed has been shown to catalyze the reverse reaction, the transfer of an acyl from PA onto CoA *in vitro* (Yamashita et al., 2007). c) Acyltransferases themselves could work as transporters of acyl-CoA or pass the activated acyl through the membrane. Nevertheless, PA biosynthesis may be dependent on transporters for glycerophospholipids, CoA or G3P. At present it appears that many questions remain to be resolved with regard to the topology of PA biosynthesis in the ER of yeast.

## Experimental procedures

*Yeast strains and media.* Strains and plasmids are listed in Table SI, PCR primers in Table SII. Cells were grown at 30°C on rich medium (YPD) or defined media (YNB plus Drop-Out Mix, USBiological, Y2025) containing 2% glucose (D, Glc), raffinose (Raf) or galactose (Gal) as a carbon source and uracil (U) and adenine (A) as required (Sherman, 2002).

*DTR analysis.* Dual topology reporters (DTR) were added to the C-terminus of C-terminally truncated versions of *GPT2* using homologous recombination and constructs were analyzed as described (Pagac et al., 2011).

*Protease protection experiments.* BY4742 cells harboring various tagged acyltransferases were grown in YNBGal to stationary phase at 24°C and microsomes were prepared. Aliquots (100 µg protein/sample) were treated with Proteinase K in buffer A (0.2 M sorbitol, 5 mM MgCl<sub>2</sub>, 0.1 M potassium phosphate, pH 7.4) supplemented with 3 mM EDTA, 1 µg ml<sup>-1</sup> Pepstatin and 10 µM E-64 for 30 min at room temperature. Reactions were stopped either by TCA precipitation or by addition of 1x EDTA-free Roche protease inhibitor cocktail plus 20 mM AEBSF, 5 mM EGTA and 20 mM PMSF.

*Gel electrophoresis and Western blotting.* Samples were incubated for 10 or 20 min at 65° or 5 min at 95 °C in reducing Laemmli sample buffer and separated by SDS-PAGE. Proteins were transferred onto a PVDF membrane using as transfer buffers 10 mM 3-(Cyclohexylamino)-1-propanesulfonic acid (CAPS), pH 11.0, 10% MeOH, 0.05% SDS or else, 25 mM Tris, 192 mM Glycine, pH8.3, 10% MeOH, with identical results.

*Cysteine accessibility assays.* Plasmid born, cysteine mutated, epitope tagged alleles of *GPT2* were expressed in haploid cells containing wild type (WT) copies of *GPT2* and *SCT1* in the genome. Microsomes were analyzed using UBI-mal and PEG-mal as recently described (Pagac et al., 2011). N-dodecyl-β-D-maltoside was used for membrane solubilization throughout because of its very low critical micelle concentration (0.12 mM) and its high capacity to preserve enzymatic activity (le Maire et al., 2000). When the Gpi8p-FLAG protein was desired as a luminal control, constructs were expressed in BY4742 *trp1Δ* containing pBF649 (FBY2280)(Figs. 3A'-D', 4A'-C'). Overexpression of WT alleles led to an increased intensity of a band with lower mobility (Fig. S2B) representing a differently phosphorylated form as was reported before (Bratschi et al., 2009), and this phosphorylated form was also observed in most mutant alleles (Fig. 3). Cells were grown in YNBRaf and Gpt2p-V5-His<sub>6</sub> was induced by addition of galactose for 30 min, because without induction the protein was not detectable in

Western blots. Assaying their capacity to complement *gpt2Δ sct1Δ* double mutants at low or high expression levels (Figs tested functionality of all cysteine mutated *gpt2* alleles. S3, S4).

Supporting information describes the origin of reagents and detailed procedures used for plasmid construction, preparation of microsomes, and preparation of UBI-mal, UBI-mal tagging of microsomes, phosphopeptide analysis and the GPAT assay.

### **Acknowledgements**

We would like to thank Dr. Laurent Falquet for helping to find cysteine-free proteins. We also thank Drs. Patrice Waridel and Mandfredo Quadroni of the Protein Analysis Facility, Center for Integrative Genomics, Faculty of Biology and Medicine, University of Lausanne, Switzerland for the analysis of the phosphopeptides of Gpt2p. This work was supported by grants 31-67188.01 and CRSI33\_125232/1 from the Swiss National Science Foundation (<http://www.snf.ch/E/Pages/default.aspx>). Author contributions: M.P., C.R. and A.C. designed research and wrote the paper. C.R., M.P., H.V., A.B. and C.D. performed research and analyzed the data.

### **Abbreviations**

DDM, n-dodecyl-β-D-maltoside; DTR, dual topology reporter; FOA, 5'-fluoroorotic acid; G3P, L-glycerol-3-phosphate; GPAT, glycerol-3-phosphate acyltransferase; LPAT, *lyso*-PA acyltransferase; PA, phosphatidic acid; PEG-mal, polyethyleneglycol-5000-maleimide; phosphosites, phosphorylated residues; TM, transmembrane helix; TNBS, trinitrobenzene sulfonic acid; TX-100, Triton X-100; UBI-mal, ubiquitin-maleimide; WT, wild type.

## References

- Alberts, B., Johnson, A., Lewis, J., Raff, M., Roberts, K., and Walter, P. (2008) In Alberts, B., Johnson, A., Lewis, J., Raff, M., Roberts, K., and Walter, P., (eds). New York: Garland Science, pp. 743-744.
- Balija, V.S., Chakraborty, T.R., Nikonov, A.V., Morimoto, T., and Haldar, D. (2000) Identification of two transmembrane regions and a cytosolic domain of rat mitochondrial glycerophosphate acyltransferase. *J Biol Chem* 275: 31668-31673.
- Bell, R.M., Ballas, L.M., and Coleman, R.A. (1981) Lipid topogenesis. *J Lipid Res* 22: 391-403.
- Bogdanov, M., Zhang, W., Xie, J., and Dowhan, W. (2005) Transmembrane protein topology mapping by the substituted cysteine accessibility method (SCAM(TM)): application to lipid-specific membrane protein topogenesis. *Methods* 36: 148-171.
- Bratschi, M.W., Burrowes, D.P., Kulaga, A., Cheung, J.F., Alvarez, A.L., Kearley, J., and Zaremberg, V. (2009) Glycerol-3-phosphate acyltransferases gat1p and gat2p are microsomal phosphoproteins with differential contributions to polarized cell growth. *Eukaryot Cell* 8: 1184-1196.
- Buck, T.M., Wagner, J., Grund, S., and Skach, W.R. (2007) A novel tripartite motif involved in aquaporin topogenesis, monomer folding and tetramerization. *Nat Struct Mol Biol* 14: 762-769.
- Cassel, M., Seppala, S., and von Heijne, G. (2008) Confronting fusion protein-based membrane protein topology mapping with reality: the *Escherichia coli* ClcA H<sup>+</sup>/Cl<sup>-</sup> exchange transporter. *J Mol Biol* 381: 860-866.
- Coleman, R., and Bell, R.M. (1978) Evidence that biosynthesis of phosphatidylethanolamine, phosphatidylcholine, and triacylglycerol occurs on the cytoplasmic side of microsomal vesicles. *J Cell Biol* 76: 245-253.

- Coleman, R.A., and Bell, R.M. (1980) Enzyme asymmetry in hepatic microsomal vesicles. Criteria for localization of luminal enzymes with proteases. *Biochim Biophys Acta* 595: 184-188.
- Coleman, R.A., and Lee, D.P. (2004) Enzymes of triacylglycerol synthesis and their regulation. *Prog Lipid Res* 43: 134-176.
- Deak, P.M., and Wolf, D.H. (2001) Membrane topology and function of Der3/Hrd1p as a ubiquitin-protein ligase (E3) involved in endoplasmic reticulum degradation. *J Biol Chem* 276: 10663-10669.
- Goder, V., and Spiess, M. (2003) Molecular mechanism of signal sequence orientation in the endoplasmic reticulum. *EMBO J* 22: 3645-3653.
- Gonzalez-Baro, M.R., Granger, D.A., and Coleman, R.A. (2001) Mitochondrial glycerol phosphate acyltransferase contains two transmembrane domains with the active site in the N-terminal domain facing the cytosol. *J Biol Chem* 276: 43182-43188.
- Guo, Z.Y., Lin, S., Heinen, J.A., Chang, C.C., and Chang, T.Y. (2005) The active site His-460 of human acyl-coenzyme A:cholesterol acyltransferase 1 resides in a hitherto undisclosed transmembrane domain. *J Biol Chem* 280: 37814-37826.
- Hedin, L.E., Ojemalm, K., Bernsel, A., Hennerdal, A., Illergard, K., Enquist, K., Kauko, A., Cristobal, S., von Heijne, G., Lerch-Bader, M., Nilsson, I., and Elofsson, A. (2010) Membrane insertion of marginally hydrophobic transmembrane helices depends on sequence context. *J Mol Biol* 396: 221-229.
- Hessa, T., Meindl-Beinker, N.M., Bernsel, A., Kim, H., Sato, Y., Lerch-Bader, M., Nilsson, I., White, S.H., and von Heijne, G. (2007) Molecular code for transmembrane-helix recognition by the Sec61 translocon. *Nature* 450: 1026-1030.

- Junne, T., Schwede, T., Goder, V., and Spiess, M. (2007) Mutations in the Sec61p channel affecting signal sequence recognition and membrane protein topology. *J Biol Chem* 282: 33201-33209.
- Kauko, A., Hedin, L.E., Thebaud, E., Cristobal, S., Elofsson, A., and von Heijne, G. (2010) Repositioning of transmembrane alpha-helices during membrane protein folding. *J Mol Biol* 397: 190-201.
- Kihara, A., Sano, T., Iwaki, S., and Igarashi, Y. (2003) Transmembrane topology of sphingoid long-chain base-1-phosphate phosphatase, Lcb3p. *Genes Cells* 8: 525-535.
- Kim, H., Melen, K., Osterberg, M., and von Heijne, G. (2006) A global topology map of the *Saccharomyces cerevisiae* membrane proteome. *Proc Natl Acad Sci U S A* 103: 11142-11147.
- Kim, H., Von Heijne, G., Yan, Q., Caputo, G.A., and Lennarz, W.J. (2003) Determination of the membrane topology of Ost4p and its subunit interactions in the oligosaccharyltransferase complex in *Saccharomyces cerevisiae*. *Proc Natl Acad Sci U S A* 100: 7460-7464.
- Kreft, S.G., Wang, L., and Hochstrasser, M. (2006) Membrane topology of the yeast endoplasmic reticulum-localized ubiquitin ligase Doa10 and comparison with its human ortholog TEB4 (MARCH-VI). *J Biol Chem* 281: 4646-4653.
- Le Gall, S., Neuhof, A., and Rapoport, T. (2004) The endoplasmic reticulum membrane is permeable to small molecules. *Mol Biol Cell* 15: 447-455.
- le Maire, M., Champeil, P., and Moller, J.V. (2000) Interaction of membrane proteins and lipids with solubilizing detergents. *Biochim Biophys Acta* 1508: 86-111.
- Lewin, T.M., Wang, P., and Coleman, R.A. (1999) Analysis of amino acid motifs diagnostic for the sn-glycerol-3-phosphate acyltransferase reaction. *Biochemistry* 38: 5764-5771.

- Marr, N., Foglia, J., Terebiznik, M., Athenstaedt, K., and Zaremborg, V. (2012) Controlling lipid fluxes at glycerol-3-phosphate acyltransferase step in yeast: unique contribution of Gat1p to oleic acid-induced lipid particle formation. *J Biol Chem* 287: 10251-10264.
- Ott, C.M., and Lingappa, V.R. (2002) Integral membrane protein biosynthesis: why topology is hard to predict. *J Cell Sci* 115: 2003-2009.
- Pagac, M., Vazquez de la Mora, H., Duperrex, C., Roubaty, C., Vionnet, C., and Conzelmann, A. (2011) Topology of 1-acyl-glycerol-3-phosphate acyltransferases SLC1 and ALE1, and related membrane bound O-acyltransferases (MBOATs) of *Saccharomyces Cerevisiae*. *J Biol Chem*
- Pitonzo, D., Yang, Z., Matsumura, Y., Johnson, A.E., and Skach, W.R. (2009) Sequence-specific retention and regulated integration of a nascent membrane protein by the endoplasmic reticulum Sec61 translocon. *Mol Biol Cell* 20: 685-698.
- Sherman, F. (2002) Getting started with yeast. *Methods Enzymol* 350: 3-41.
- Shindou, H., and Shimizu, T. (2009) Acyl-CoA:lysophospholipid acyltransferases. *J Biol Chem* 284: 1-5.
- Slabas, A.R., Kroon, J.T., Scheirer, T.P., Gilroy, J.S., Hayman, M., Rice, D.W., Turnbull, A.P., Rafferty, J.B., Fawcett, T., and Simon, W.J. (2002) Squash glycerol-3-phosphate (1)-acyltransferase. Alteration of substrate selectivity and identification of arginine and lysine residues important in catalytic activity. *J Biol Chem* 277: 43918-43923.
- Strahl-Bolsinger, S., and Scheinost, A. (1999) Transmembrane topology of pmt1p, a member of an evolutionarily conserved family of protein O-mannosyltransferases. *J Biol Chem* 274: 9068-9075.
- Tamada, T., Feese, M.D., Ferri, S.R., Kato, Y., Yajima, R., Toguri, T., and Kuroki, R. (2004) Substrate recognition and selectivity of plant glycerol-3-phosphate acyltransferases

(GPATs) from *Cucurbita moscata* and *Spinacea oleracea*. *Acta Crystallogr D Biol Crystallogr* 60: 13-21.

Wilkinson, B.M., Critchley, A.J., and Stirling, C.J. (1996) Determination of the transmembrane topology of yeast Sec61p, an essential component of the endoplasmic reticulum translocation complex. *J Biol Chem* 271: 25590-25597.

Yamashita, A., Nakanishi, H., Suzuki, H., Kamata, R., Tanaka, K., Waku, K., and Sugiura, T. (2007) Topology of acyltransferase motifs and substrate specificity and accessibility in 1-acyl-sn-glycero-3-phosphate acyltransferase 1. *Biochim Biophys Acta* 1771: 1202-1215.

Zaremborg, V., and McMaster, C.R. (2002) Differential partitioning of lipids metabolized by separate yeast glycerol-3-phosphate acyltransferases reveals that phospholipase D generation of phosphatidic acid mediates sensitivity to choline-containing lysolipids and drugs. *J Biol Chem* 277: 39035-39044.

Zhang, Y.M., and Rock, C.O. (2008) Thematic review series: Glycerolipids. Acyltransferases in bacterial glycerophospholipid synthesis. *J Lipid Res* 49: 1867-1874.

Zheng, Z., and Zou, J. (2001) The initial step of the glycerolipid pathway: identification of glycerol 3-phosphate/dihydroxyacetone phosphate dual substrate acyltransferases in *Saccharomyces cerevisiae*. *J Biol Chem* 276: 41710-41716.

## Figure legends

**Fig. 1. Biosynthesis of phosphatidic acid in yeast.** Enzymes containing the Pfam motif PF01553 are in red.

**Fig. 2. Probing Gpt2p using a dual topology reporter.** **A**, TM probability for Gpt2p sequence as predicted by TMHMM. Positions of conserved motifs I to IV are indicated by yellow bars. **B**, TM predictions by the 5 TOPCONS algorithms SCAMPI-seq, SCAMPI-msa, PRODIV, PRO and OCTOPUS (a-e) and the TOPCONS global prediction (f), which latter takes into account algorithms a) – e), as well as the  $\Delta G_{mi}$  and ZPRED algorithms, which are not shown. Potential TMs are numbered 1-6 in line a). Sequences predicted to be luminal and cytosolic are in blue and red, respectively. **C**, Gpt2p topology inferred from our data is indicated by the solid line, using the color coding of Fig. 2B; loop topologies inferred only by the TOPCONS global prediction are indicated by dotted lines.  $\Delta G_{mi}$  obtained from the  $\Delta G$  predictor are indicated in green. Orange arrowheads indicate positions of the 8 natural Cys. The C-terminus of Gpt2p was found to be cytosolic in a global DTR topology study (Kim et al., 2006). Light blue rhomboids indicate phosphorylated amino acids identified by phosphopeptide analysis (Fig. S6). **D**, DTRs were inserted at the positions indicated by green arrows in panel C. The various Gpt2p-DTR proteins were expressed in STY50 and microsomal proteins were analyzed by Western blotting using anti-HA antibody before and after endoglycosidase H (Endo H) treatment (left panels). The location of the DTRs was also evaluated by probing the cells' ability to grow on histidinol, the substrate of His4p (right panels).

**Fig. 3. Cysteine accessibility indicates luminal orientation of loop L1-2 of Gpt2p.** **A-D**, cysteine accessibility in Gpt2p in absence or presence of detergents (Det; DDM = D, SDS = S) was probed with UBI-mal (Ubi) in microsomes of BY4742 *trp1* $\Delta$  harboring Gpt2p-V5-His<sub>6</sub> alleles containing only the cysteines denoted above each panel. Gpt2p was revealed with anti-V5 antibody. Panel **A** also shows the functionality of Gpt2p-5CS-C77-254-297-V5-His<sub>6</sub> by showing the growth of a tetratype progeny containing single ( $\Delta$ ) and double (2 $\Delta$ ) deletions of *GPT2* and *SCT1* on glucose and galactose. This is also shown for all constructs in Fig. S3. **A'-D'**, cells analyzed in panels A-D contained also a plasmid harboring Gpi8p-FLAG (pBF649) and samples were in parallel Western blotted with anti-Kar2p and anti-FLAG. The data indicate that all microsomes were intact, as no cysteine modification of these luminal controls was observed in the absence of detergent.

**Fig. 4. Cysteine accessibility indicates cytosolic orientation of loop L2-3 of Gpt2p.** **A-C**, cysteine accessibility was probed as in Fig. 3, but in *gpt2* alleles derived from Gpt2p-5CS-C77-

254-297-V5-His<sub>6</sub> harboring artificial cysteine substitutions in loop L2-3. **A'-C'**, intactness of microsomes used in panels A-C was tested as in Fig. 3A'-D'.

**Fig. 5. Probing Gpt2p using epitope insertions.** **A-C**, microsomes from WT cells containing Gpt2p-235-HA (panel **A**), Gpt2p-235-VSVG (panel **B**) or Gpt2p-412-VSVG (panel **C**) having an HA or VSVG tag inserted after amino acid 235 or 412, respectively, were treated in two independent experiments (left and right panels) with the indicated amounts of proteinase K (PK) in the presence or absence of 0.5% TX-100 (panels **A, C**) or 2% n-dodecyl- $\beta$ -D-maltoside (DDM)(panel **B**). Protease was inactivated and extracts were analyzed by Western blotting using anti-HA or anti-VSVG antibodies. Samples run in lanes marked with \*, \*\* or \*\*\* were run in parallel in Fig. S5B. **D**, microsomes from cells expressing the Gpt2p-412-HA construct were incubated with proteinase K at concentrations ranging from 0 to 3  $\mu$ g, in the presence or absence of 0.5% TX-100. Gpt2p was detected as above. In panels **A** and **D**, lanes 9, the protease was pre-inhibited with protease inhibitors before being added to detergent-permeabilized microsomes. **E**, the extracts treated with 0.045 and 11  $\mu$ g proteinase K in panel C (lanes 1, 2, 3, 6, 13, 16) were probed with anti-Gpi16p antibody, which recognizes the lumenally located Gpi16p subunit of the GPI transamidase.

**Fig. 6. GPAT activity of microsomes is sensitive to trinitrobenzene sulfonic acid only in the presence of detergent.** **A**, microsomes of *sct1* $\Delta$  cells were preincubated for 1 h on ice-water in the absence (-) or presence (+) of 0.1% TX-100 and 0 (-), 0.125% (+), or 0.625% (++) TNBS (w/v). Then, GPAT activity was measured by adding [<sup>14</sup>C]-G3P, then, the lipids were extracted and analyzed by TLC and phosphorimaging. Lane 2 shows a reaction, where boiled microsomes were used. **B**, reports the sum of counts in *lyso*-PA and PA for each of the lanes (1 - 7) in the experiment of panel A and 3 other, identical GPAT assays. 100% corresponds to the mean of incorporation into lipids in condition 1 and amounts to 7'330 cpm or 1.6% of the radioactivity added to microsomes. Standard deviations are indicated.

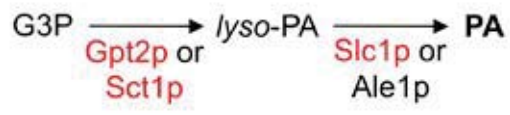


Fig. 1

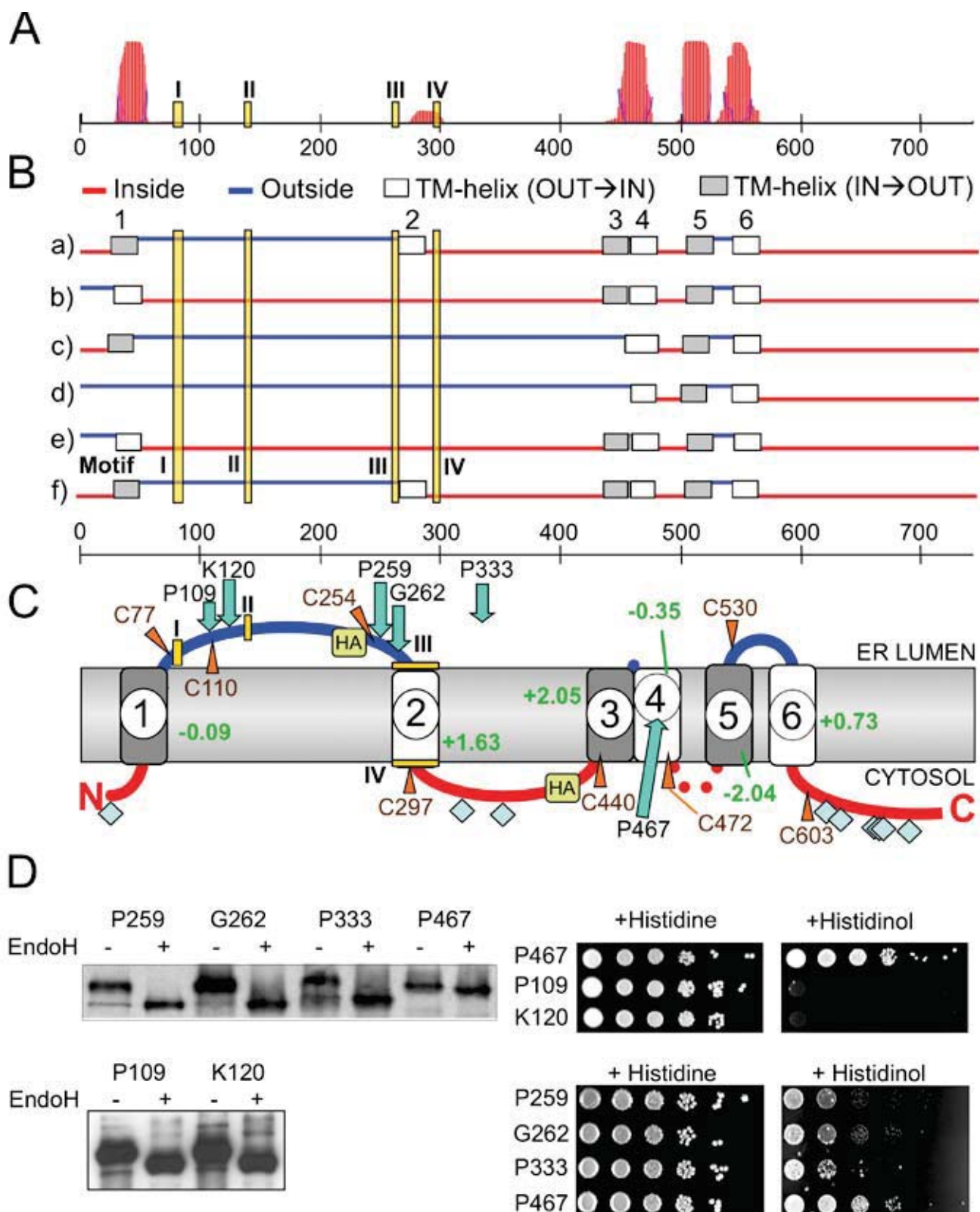


Fig. 2A-D

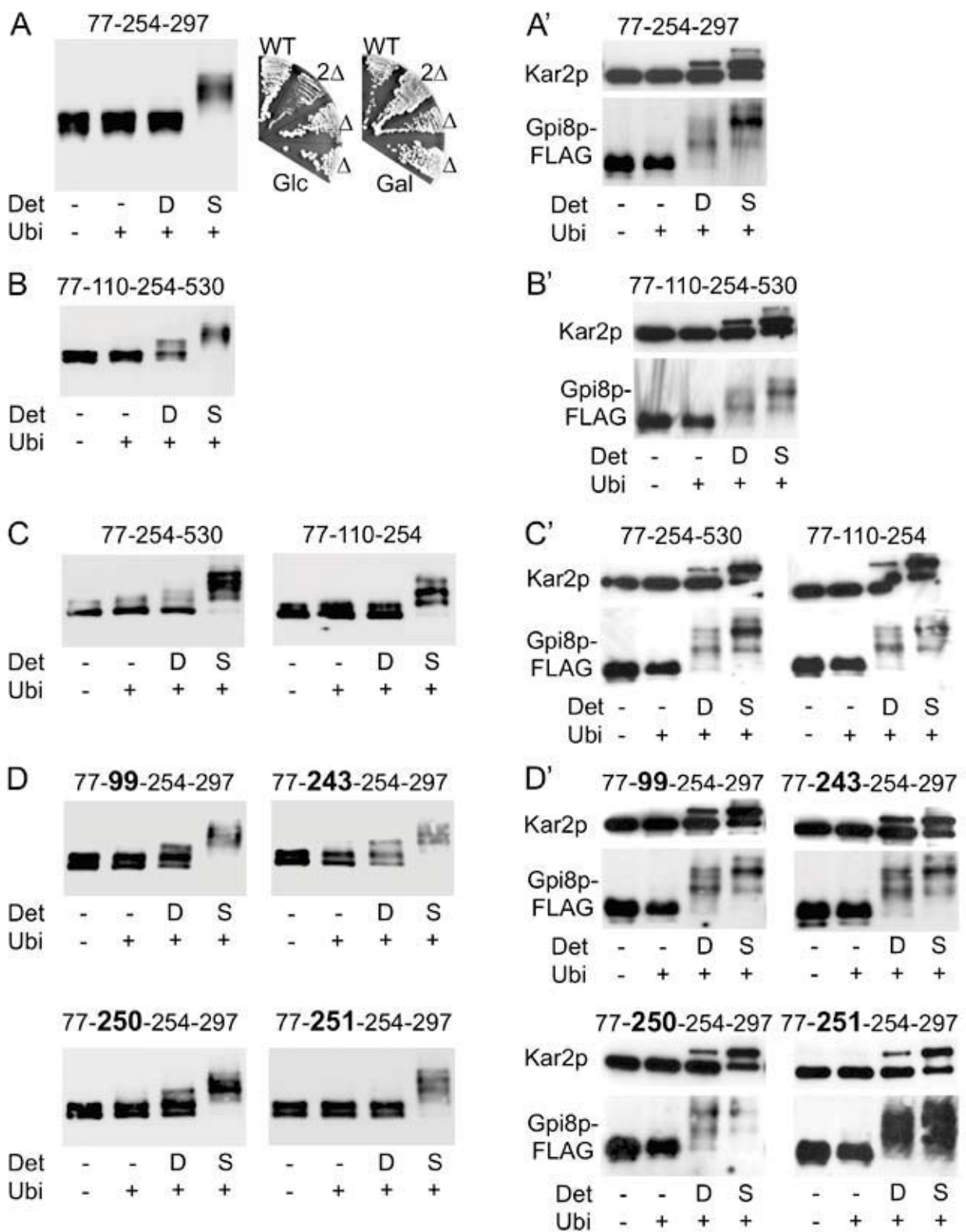


Fig. 3A-D, A'-D'

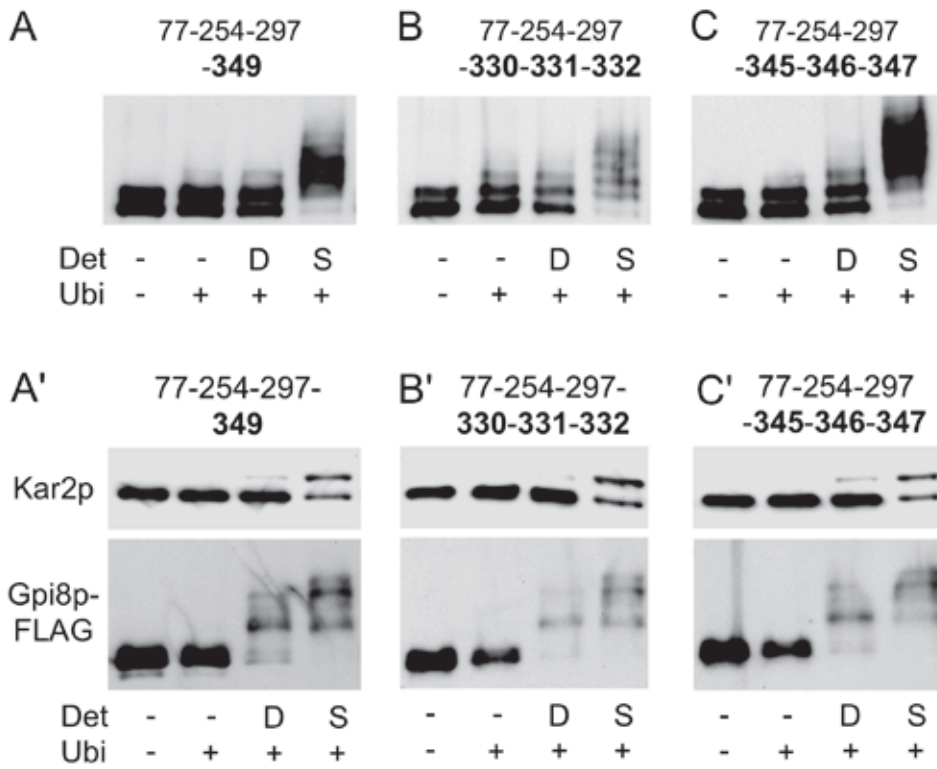


Fig. 4A-C, A'-C'

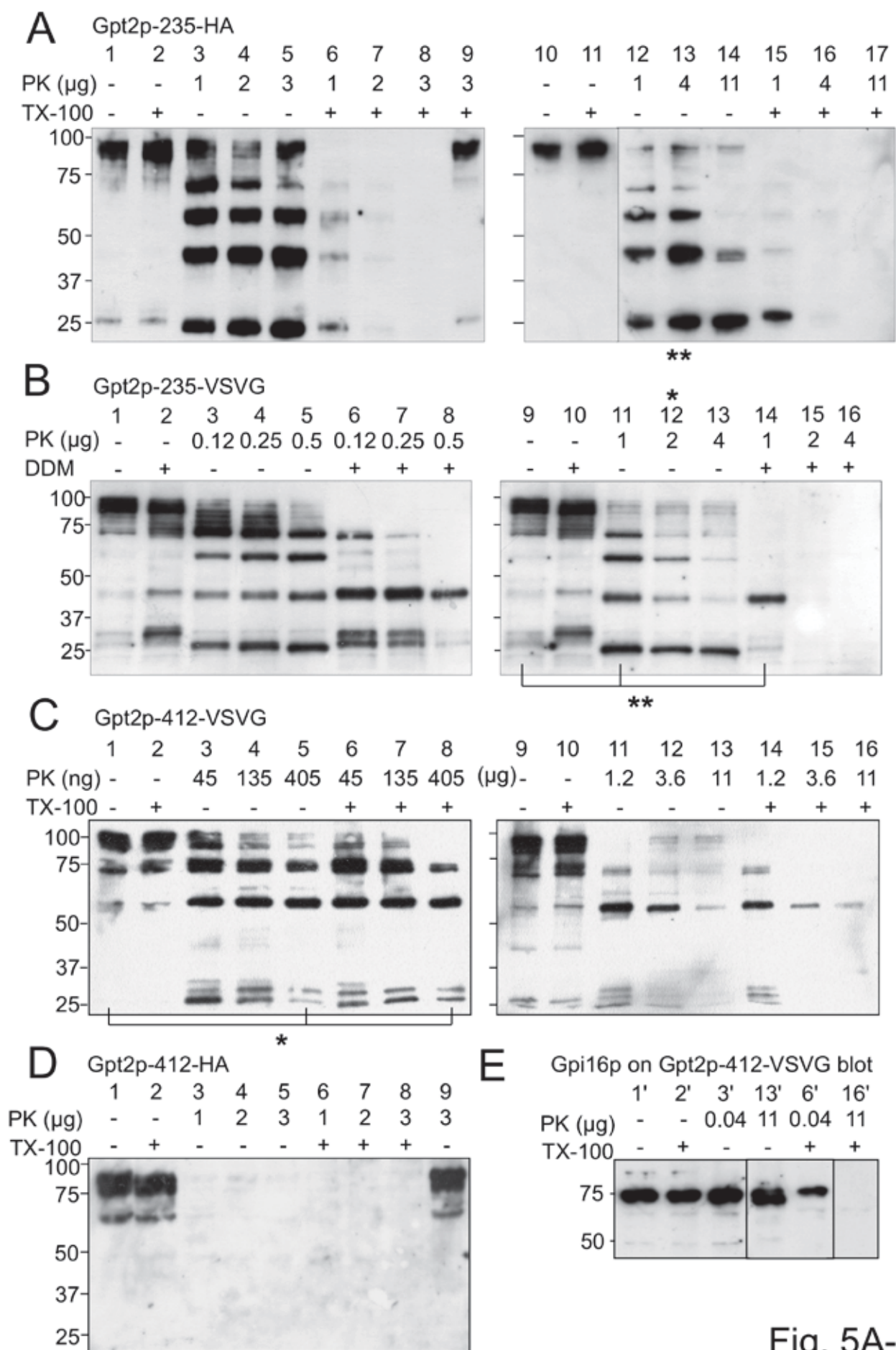


Fig. 5A-E

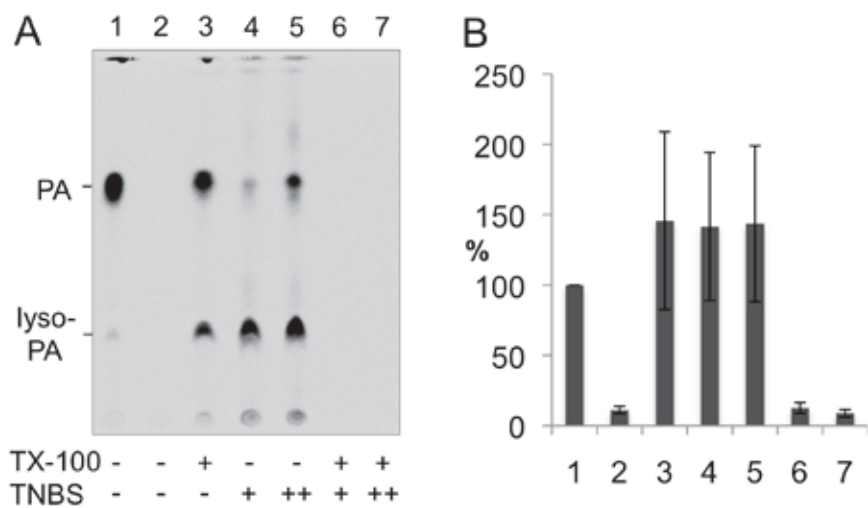


Fig. 6A, B